A novel derivative of quinazoline, WYK431 induces G_2/M phase arrest and apoptosis in human gastric cancer BGC823 cells through the PI3K/Akt pathway

TIAN-EN WANG, YONG-KANG WANG, JING JIN, BAI-LING XU and XIAO-GUANG CHEN

Department of Pharmacology, State Key Laboratory of Bioactive Substance and Function of Natural Medicines, Institute of Materia Medica, Chinese Academy of Medical Sciences and Peking Union Medical College, Beijing 100050, P.R. China

Received February 24, 2014; Accepted April 28, 2014

DOI: 10.3892/ijo.2014.2458

Abstract. WYK431, a novel synthetic quinazoline derivative, showing potent inhibition of proliferation activity against a broad spectrum of human cancer cell lines. We investigated the anticancer effects of WYK431 on BGC823 cells both *in vitro* and *in vivo*. The results showed that WYK431 inhibited proliferation, arrested the cell cycle at the G_2/M phase, which was related to CDK1 and CDC25C, and induced apoptosis associated with activation of caspase-3 and caspase-9 rather than caspase-8 in BGC823 cells. Treatment of BGC823 cells with WYK431 resulted in upregulation of Bax, release of cytochrome c from the mitochondria to the cytosol and disruption of mitochondrial membrane potential. Western blot analysis showed that WYK431 downregulated the levels of the PI3K/Akt signaling pathway. Moreover, WYK431 effectively suppressed tumor growth in xenograft models in BALB/c athymic nude mice without major side action. TUNEL analysis showed that WYK431 induced BGC823 cell apoptosis *in vivo*. Collectively, WYK431 is a novel small molecule agent which inhibits BGC823 cell proliferation inducing G_2/M phase arrest and apoptosis via the mitochondrial apoptotic pathway. To assess its potential as a promising anticancer agent requires further investigation.

Introduction

Gastric cancer (GC) is the second leading cause of cancer death in the world, and especially in Asian countries, including China (1,2). Conventional treatment modalities including surgery, radiotherapy and chemotherapy play a role mainly in patients at early stage. However, these modalities are far from satisfactory for patients with advanced gastric cancer, with considerable treatment-associated toxicity and dismal overall survival time (3,4). With better understanding of the biology and underlying molecular mechanism of carcinogenesis, new therapeutic approaches are needed for advanced gastric cancer treatment.

Increasing evidence demonstrates that PI3K signaling pathway regulates various cellular processes including proliferation, cell cycle progression, apoptosis, migration and metabolism (5,6). The dysregulation of PI3K/AKT pathway has been recently found to be involved in the pathogenesis of various human cancers such as gastric, colon, breast, pancreatic and prostate cancer (7). PI3K catalyzes the phosphorylated of 3-hydroxyl position of PIP2 (phosphatidylinositol 4,5-diphosphate) to PIP3 (phosphatidylinositol 3,4,5-triphosphate) (8,9). PI3Ks are grouped into three classes (I, II and Ⅲ) with regulatory subunit for each, based on their respective structural characteristics and substrate specificity (10,11). The most extensively studied PI3Ks are class I PI3Ks, especially class IA PI3Ks which are composed of heterodimers of a p85 regulatory subunit and a p110 catalytic subunit (12). The dysregulation of p110α has been observed in many human cancers such as gastric, colon, ovarian, hepatocellular and breast carcinoma (13-16).

The Akt family, also well known as protein kinase B, is one of the major downstream mediators of the PI3K pathway. Akt plays very important roles in various cellular functions such as cell cycle progression, proliferation, apoptosis, migration and angiogenesis (17). Akt gene amplification has been observed in a number of human cancers such as gastric, breast and ovarian cancer. In addition to amplification, recent studies have shown that elevation of Akt activities is associated with a poor prognosis in human cancers. Whereas tumor suppressor phosphatase and tensin homologue (PTEN) negatively regulates the PI3K signals (18). The control of cell growth by PI3K/Akt pathway via regulating cell proliferation, cell cycle progression and apoptosis implicates a crucial role of this pathway in carcinogenesis and cancer development. Therefore,

Correspondence to: Professor Xiao-Guang Chen, Department of Pharmacology, State Key Laboratory of Bioactive Substance and Function of Natural Medicines, Institute of Materia Medica, Chinese Academy of Medical Sciences and Peking Union Medical College, Beijing 100050, P.R. China
E-mail: chxg@imm.ac.cn

Key words: WYK431, human gastric cancer, mitochondrial apoptotic pathway

PI3K is a potential target for cancer prevention and therapy. Inhibition of PI3K/Akt pathway in gastric cancer seems to be a promising strategy for the treatment.

Cell cycle progression is promoted by the activity of phase-specific kinase complexes composed of cyclins and cyclin-dependent kinases (19). It consists of four distinct phases: G_1 phase, S phase (synthesis), G_2 phase and M phase (mitosis). From G_2 phase to M phase, it requires the activation of cyclin B/CDK1, which push the cells through the G_2 checkpoint and are regulated by CDC25C (20).

There is ample evidence that cancer is characterized by uncontrolled cellular growth and proliferation, and therefore inducing cancer cells into apoptosis is one of the important therapeutic intervention approaches in cancer (21,22). Apoptosis is characterized by a number of morphological and biochemical features, such as cell shrinkage, nuclear DNA fragmentation and membrane blebbing (23,24). Apoptosis is mediated through two main routes the death receptor pathway (extrinsic) and the mitochondrial pathway (intrinsic). In the death receptor pathway, Fas/CD95 combines with its ligand FasL recruits procaspase-8 and activates downstream effectors caspase-3 and/or caspase-7 (25). Upon activation of the mitochondrial pathways, the change of mitochondrial membrane results in release of cytochrome c, and caspase-9 activation. In turn, activated caspase-9 leads to cleavage of the executioner caspase-3 and caspase-7, and finally results in chromatin condensation, DNA laddering and formation of apoptotic bodies (26).

Quinazoline derivatives have been reported to possess a wide range of therapeutic activities including anticancer (27), anti-inflammation (28), anti-bacterial (29), antihypertension (30). Recently, some quinazoline derivatives have been reported to have antitumor effects in several human tumor cell lines by our research group (31,32). With a goal of developing a more effective derivative, a series of quinazoline derivatives were synthesized and screened. Among them, methyl 4-([6-chloro-2-([1'-methyl-(1,4'-bipiperidin)-4-yl] amino)quinazolin-4-yl]amino)benzoate (WYK431) displayed the most potent antitumor activity and induced apoptosis *in vitro*. However, molecular mechanisms of action underlying WYK431 against cancer remain unknown. Therefore, investigating the molecular mechanisms of WYK431 is urgent for the development of WYK431 as a potential anticancer agent. In this study, we demonstrate that WYK431 inhibits BGC823 cells proliferation, induces G_2/M arrest and apoptosis though intrinsic apoptotic pathway *in vitro* and suppresses tumor growth *in vivo*.

Materials and methods

Materials. DMSO,3-(4,5-Dimethylthiazol-2-yl)-2,5-diphenyltetrazolium bromide (MTT), propidium iodide (PI), Triton X-100 and rhodamine-123 (Rh-123) were purchased from Sigma Chemical Co. (St. Louis, MO, USA). The Annexin V-FITC apoptosis detection kit was purchased from KoradBio (Beijing, China). The primary antibodies against caspase-3, caspase-8, caspase-9, Bcl-2, Bax, Akt, p-Akt (Ser473), CDK1, Cyclin B1, CDC25C, p85 and p110α were purchased from Cell Signaling Technology (Beverly, MA, USA). Antibodies against cytochrome c and β-actin were purchased from Santa Cruz Biotechnology (Santa Cruz, CA, USA). TUNEL (terminal deoxynucleotidyl transferase mediated dUTP nick end-labeling) assay kit was purchase from Millipore (CA, USA). RPMI-1640 or DMEM were obtained from Gibco BRL Co. (Grand Island, NE, USA). All of the chemicals employed in this study were culture grade and analytic purity.

WYK431 was synthesized and supplied as a yellow solid by Institute of Materiel Medica, Chinese Academy of Medical Sciences and Peking Union Medical College. Its structural formula is shown in Fig. 1A. WYK431 was dissolved in dimethyl sulfoxide (DMSO) to give a 5 mM stock solution, which was stored at 4˚C and diluted with the relevant medium for the *in vitro* experiments. For the *in vivo* studies, WYK431 was solubilized in 20% PEG (Beijing Chemical Works, Beijing, China) to yield stock solutions of 2, 1 and 0.5 mg/ml, and stored at -20˚C.

Cell culture. The following human carcinoma cell lines were obtained from American Type Culture Collection (ATCC, Manassas, VA, USA): MCF7 cells; HepG2 cells; A2780 cells; A549 cells; HCT 116 and T47D. BGC823 and BGC803 purchased from Cell Culture Center of Institute of Basic Medical Sciences, Chinese Academy of Medical Sciences. Cells were cultured in DMEM or RPMI-1640 media containing 10% FBS and 1% antibiotics (penicillin and streptomycin) under humidified conditions with 5% CO_2 at 37˚C.

Cell viability assay. MTT assay was used to measure the cell viability after WYK431 treatment. Briefly, the cells ($3x10^3$ cells/well) were seeded in a 96-well plate and cultured for 24 h. After WYK431 treatment, the drug containing medium was removed and replaced by fresh medium. MTT solution (100 μl of 0.5 mg/ml) was added per well and incubated for another 4 h at 37˚C, then the supernatant fluid was removed and DMSO was added 150 μl to each well. The plates were gently agitated until the color reaction was uniform. The OD570 was measured using a microplate reader (Wellscan MK3, Labsystems Dragon), and the IC_{50} values were detected.

Cell cycle analysis. Cells were seeded in 6-well plates at the density of $2x10^5$/well and cultured for 24 h, followed by indicated concentrations WYK431 treatment for 24 h. Then, the cells were incubated with 1 ml of a solution containing 50 μg/ml propidium iodide (PI) and 0.1% Triton X-100 for 10 min in the dark and then immediately analyzed by flow cytometer.

Morphological analysis after DAPI staining. To investigate the apoptosis induction effect of WYK431, morphological analysis by DAPI staining was performed. Briefly, BGC823 cells ($1x10^5$) were seeded in 6-well plates for 24 h, followed by WYK431 treatment for 24 h. After fixed with 70% of ethanol, the cells were rinsed with PBS. Then cells were examined with an inverted fluorescence microscopy after staining with DAPI.

Apoptosis analysis by flow cytometry (FCM). To further confirm the apoptosis-induced effect by WYK431, we analyzed the percentage of the early apoptotic cells using an Annexin V-FITC apoptosis detection kit according to

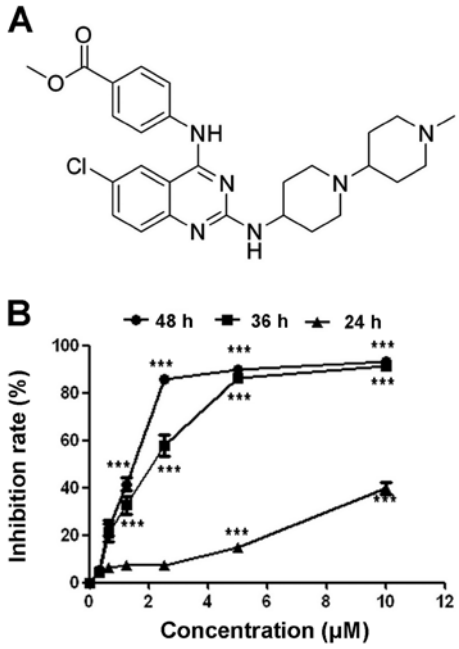

Figure 1. The chemical structure and the effect of WYK431 on BGC823 cell viability. (A) The chemical structure of WYK431. (B) The cells were treated with WYK431 for 24, 36 or 48 h. The cell viability was determined by MTT assay (***P<0.001 vs. the control group).

the manufacturer's instructions. Briefly, cells were seeded in 6-well plates at the density of $2x10^5$/well and cultured for 24 h, followed by WYK431 treatment for 36 h, and then collected and washed with cold PBS twice. Cells were stained with an Annexin V-FITC apoptosis detection kit following the manufacturer's instructions and then immediately examined by a flow cytometer.

Analysis of the mitochondrial membrane potential. The mitochondrial transmembrane potential ($\Delta\Psi m$) of cells treated with WYK431 or medium alone was measured using the rhodamine 123 (Rh123) as previously described (33). Cells were seeded in 6-well plates at the density of $2x10^5$/well and cultured for 24 h. After WYK431 treatment for 24 h, the cells were incubated with 5 μg/ml Rh123 at 37˚C in the dark for 30 min. Then fluorescence emitted from the Rh123 was measured by FCM.

Western blot analysis. Western blot analysis was performed as previously described (34). Briefly, the cells were treated with WYK431 for various concentrations and lysed with protein lysis buffer. Protein concentration was determined with Bio-Rad Protein Assay kit (Bio-Rad Laboratories), dissolved in 5X SDS sample buffer and denatured. The samples were separated according to molecular weight on 8-15% sodium dodecyl sulfate-polyacrylamide (SDS-PAGE) gel and electroblotted onto a polyvinylidene difluoride (PVDF) membrane. Membranes were blocked for 1 h in 5% dried milk in TBST at room temperature with rotation. Then membranes were incubated overnight at 4˚C with the respective primary antibodies diluted in blocking buffer. The membrane blots were washed thrice for ~10 min with TBST and incubated with appropriate horseradish peroxidase-conjugated species-specific antibody diluted in blocking buffer for 2 h at room temperature with rotation. After 3 additional washes, the immunoreactive bands were visualized using the enhanced chemiluminescence method.

Analysis of cytochrome c in cytosolic and mitochondria extracts. For detection of cytochrome c, the cytosolic and mitochondria fractions were prepared as described previously (35). Briefly, BGC823 cells were treated with WYK431 at various concentrations for 24 h and then harvested by centrifugation at 800 x g at 4˚C for 15 min. After washing with ice-cold PBS for 3 times, the cell pellets were resuspended in HEPES buffer (20 mM HEPES, 10 mM KCl, 1.5 mM $MgCl_2$, 1 mM EDTA, 1 mM EGTA, 1 mM DTT, 0.1 mM PMSF, pH 7.5) containing 250 mM sucrose, homogenized with a homogenizer and centrifugation at 800 x g at 4˚C for 15 min. The supernatants were centrifuged at 10000 x g for 15 min at 4˚C, and the mitochondria pellets were dissolved in SDS sample buffer (25 μl), subjected to 15% SDS polyacrylamide gel electrophoresis and analyzed by immunoblotting with monoclonal antibodies against cytochrome c (Santa Cruz Biotechnology). Aliquots of supernatant were also analyzed for cytochrome c expression by western blotting.

Immunofluorescence staining. To assess whether WYK431 induces cytochrome c release from mitochondria to cytosol, immunofluorescence staining was performed, and the cells were treated with 5 μM WYK431 for 24 h. To identify the location of cytochrome c, the cells were fixed with freshly prepared buffer containing 4% formaldehyde for 15 min at 37˚C. After fixation, the cells were permeabilized with buffer containing 2% Triton X-100 for 10 min at room temperature. The cells were blocked with 5% goat serum in PBS and incubated overnight with the anti-cytochrome c monoclonal antibody (diluted 1:100 in 5% goat serum, Santa Cruz Biotechnology). After three washes, cells were incubated with Alexa Fluor 488® goat anti-mouse IgG (H+L) (diluted 1:100 in 5% goat serum, Molecular Probe) for 1 h at room temperature in the dark followed by rinsing the cells three times in PBS for 5 min each. In addition, the cells were stained with DAPI for 5 min in the dark. The coverslips were mounted onto the slides using the Dako® Fluorescence Mounting Medium (Dako, Glostrup, Denmark) and fluorescence images were recorded using fluorescence microscopy.

Tumor xenograft experiments. Seven-week-old BALB/c athymic nude mice (Beijing Animal Center, Beijing, China) were established as a xenograft tumor model of BGC-823 in present study. BGC-823 cells ($1x10^7$) were inoculated in the dorsal area of mice. After 3 weeks of growth, the tumors were chopped into 3x3x3 mm^3 pieces and implanted by subcutaneous injection in the dorsum of the mice with a gange trocar. When tumors grew to approximately 100 mm^3, the nude mice bearing a tumor were randomly assigned into four groups (6 per group) and injected intraperitoneally with the following treatments, respectively: i) 20 mg/kg WYK431, ii) 10 mg/kg WYK431, iii) 5 mg/kg WYK431, iv) Vehicle. The systemic therapy started on day 7 and was repeated every three days for 12 days. Tumor volumes were assessed by bilateral Vernier caliper measurement every three days and calculated

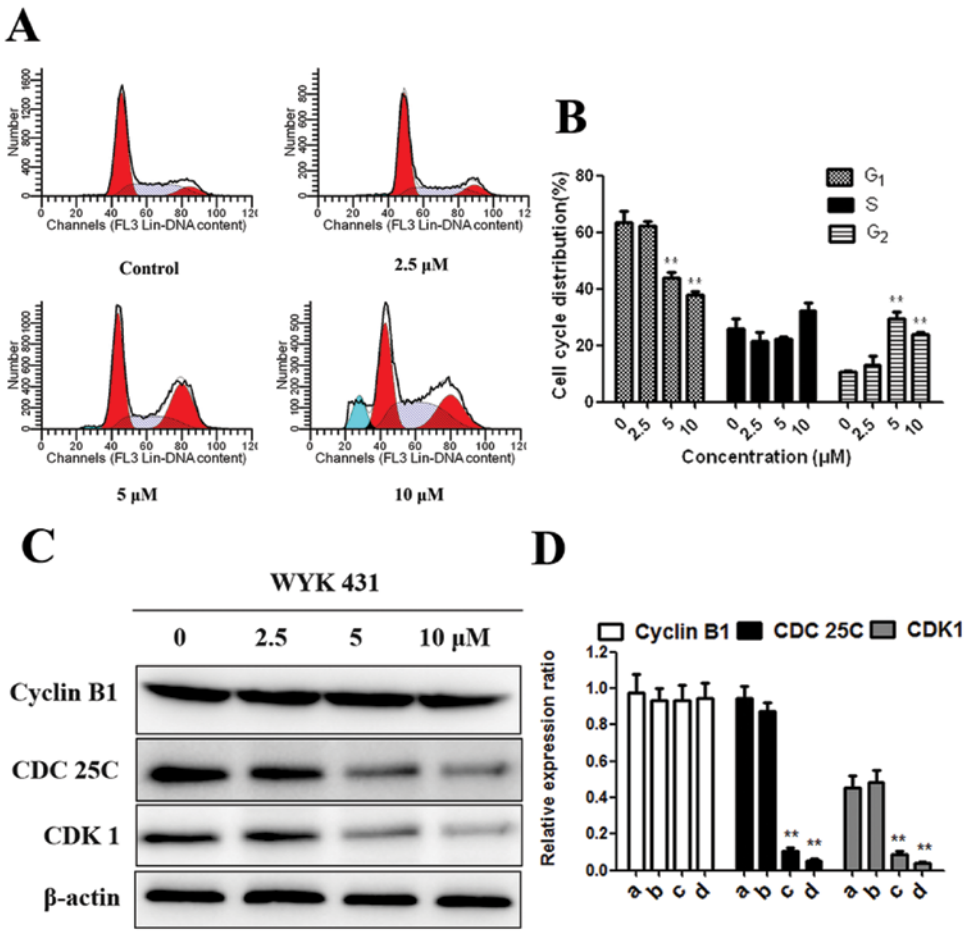

Figure 2. Effect of WYK431 on cell cycle distribution on BGC823 cancer cells. (A and B) Cells were treated with 0, 2.5, 5 and 10 μM WYK431 for 24 h. Data are presented as the means ± SD of three independent experiments. WYK431-treated group compared with the control group of G_2/M phase. **P<0.01. (C and D) Proteins involved in G_2/M phase were modulated by WYK431. BGC823 cells were treated with WYK431 at indicated concentrations for 24 h and the whole cell lysates were prepared and analyzed by immunoblotting. Bars represent the densitometric intensity of the indicated protein bands, using image analyzing software. Results are representative of three individual experiments. Control (a), WYK431 2.5 μM (b), WYK431 5 μM (c), WYK431 10 μM (d). *P<0.05 and **P<0.01 vs. control.

according to the following equation: [tumor volume = $(\text{width})^2$ x length/2)]. Body weight was measured every three days and clinical symptoms, including mortality, body weight, movement and gross findings, were observed daily. The mice were fasted overnight after the last administration and sacrificed. Blood was collected for hematological analysis using a Nihon Kohden MEK-5216K automatic hematology analyzer. All experiments were carried out on animals in compliance with the guidelines set by the institute's Animal Care and Use Committee.

TUNEL detection. The analysis of apoptotic cells in tumor tissue was conducted by TUNEL staining by an apoptotic cell detection kit (Minipore). Images of the sections were taken by a fluorescence microscope.

Statistical analysis. The data are presented as the means ± SE. Statistical analysis was performed using SPSS 13.0 software (Chicago, IL, USA). Statistical significance of the difference between groups was analyzed by one-way analysis of variance. P<0.05 was considered statistically significant.

Results

Effects of WYK431 on cell viability. The effect of WYK431 on cell viability was detected using MTT assay. Our results showed WYK431 markedly reduced the viability of a panel of cancer cell lines with IC_{50} ranged from 2 to 10 μM (Table I). BGC8-23 cell line was the most sensitive to WYK431 treatment. Furthermore, we investigated the time-and concentration-dependent effects of WYK431 on BGC823 cell viability. As shown in Fig. 1B, the IC_{50} was 1.9±0.3 and 2.24±0.4 after WYK431 treatment for 48 and 36 h, respectively. The results indicated that WYK431 inhibited the proliferation of BGC823 cells in a time- and concentration-dependent manner.

WYK431 treatment induces G_2/M phase arrest in BGC823 cells. To investigate the mechanism responsible for WYK431-induced inhibition of cell growth, flow cytometric analysis was performed after treatment of BGC823 with indicated concentrations of WYK431 for 24 h. As can be seen in Fig. 2A, cells treated with 5 μM WYK431 increased cells population at G_2/M phase compared with control cells. In addition, at 10 μM of

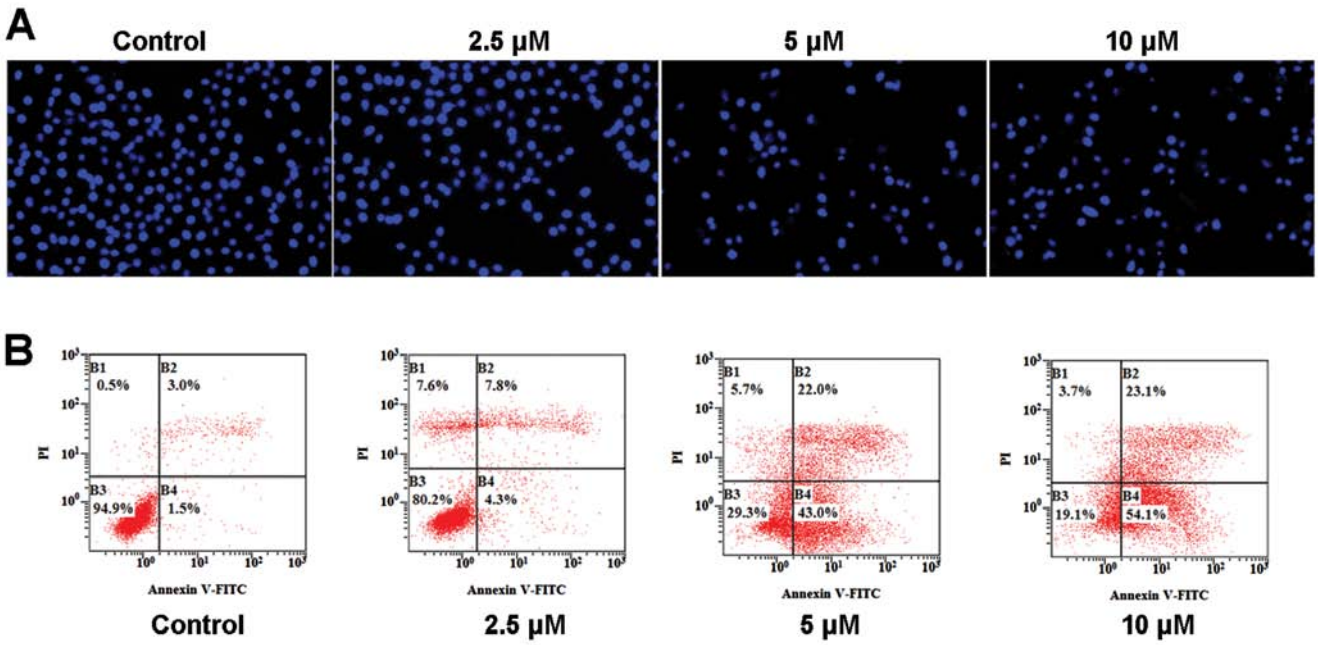

Figure 3. Effect of WYK431 on cell morphological changes and apoptosis in BGC823 cells. (A) BGC823 cells were incubated with WYK431 for 24 h. The fluorescence microscopic appearance of DAPI-stained nuclei (x400). (B) Annexin V flow cytometric analysis of apoptosis on BGC823 cells. Cells were treated with indicated concentrations of WYK431 for 36 h and the level of apoptosis was assessed using the Annexin V-FITC/PI staining. The early apoptotic cells were counted from the lower right quadrant, and the late apoptotic cells were counted from the upper right quadrant. Data are representative of three parallel experiments.

Table I. The effects of 431 on tumor cells viability.

Cell line	Cell type	IC_{50} (μM)
BGC823	Human gastric carcinoma cell line	2.16
BGC803	Human gastric carcinoma cell line	2.59
A549	Human lung adenocarcinoma cell line	3.12
$HepG_2$	Human hepatoblastoma cell line	6.66
A2780	Human ovarian carcinoma cell line	7.22
T47D	Human breast adenocarcinoma cell line	4.73
MCF7	Human breast adenocarcinoma cell line	4.68
HCT116	Human colorectal carcinoma cell line	>10

MTT assay was employed to detect the cell viability. Each cell line was treated with various concentrations of WYK431 for 48 h, respectively. Data represent the mean values from three independent experiences.

WYK431, the G_2/M phase population started to decrease, but the sub-G_1 phase population slightly increased (Fig. 2A and B). To further elucidate the mechanism of 431-induced cell cycle arrest at G_2/M phase, the expression of CDK1, CDC25C and Cyclin B1 all of which participated in G_2/M phases were detected by western blot assay. It was observed that the expression of CDK1 and CDC25C were significantly decreased at 5 and 10 μM, whereas the expression of Cyclin B1 was not changed after treatment of BGC823 cells with WYK431 for 24 h (Fig. 2C and D). These results indicated that WYK431-induced G_2/M phase arrest related to the expression levels of CDK1 and CDC25C.

WYK431 treatment induces apoptosis in BGC823 cells. We explored whether treatment of BGC823 cells with WYK431 resulted in morphological changes. Fluorescence microscopic examination of DAPI stained cells was performed. Treatment with WYK431 showed features of apoptotic cells such as a bright blue fluorescent condensed nuclei and apoptotic bodies (Fig. 3A).

Furthermore, apoptosis was measured using an Annexin V-FITC apoptosis detection kit via flow cytometry. This combination allows the differentiation among viable cells (AV^-/PI^-), early phase apoptotic cells (AV^+/PI^-), late phase apoptotic cells (AV^+/PI^+) and necrotic cells (AV^-/PI^+). After treatment with 2.5, 5 and 10 μM WYK431 for 36 h, the percentages of apoptotic cells was 12.1, 65 and 77.2%, respectively (Fig. 3B). These results indicated that WYK431 could induce apoptosis and death in BGC823 cells in a dose-dependent manner *in vitro* (Table II).

WYK431 treatment induces apoptosis via the intrinsic pathway. To further confirm the induction of apoptosis with WYK431 treatment, we examined caspase-3, caspase-8 and caspase-9 expression levels in BGC823 cells after WYK431 treatment for 24 h by western blot analysis. As shown in Fig. 4, procaspase-3, and procaspase-9 decreased significantly after WYK431 exposure for 24 h in BGC823 cells and the levels of cleaved caspase-3 and -9 increased, but no change of caspase-8 was observed. According to the results, we propose that WYK431 triggers apoptosis trough the intrinsic pathway.

WYK431 induces cytochrome c released. Previously, it has been reported that during mitochondrion-mediated apoptotic pathway, the release of cytochrome c from mitochondria into cytosol promotes caspase activation (36). Therefore,

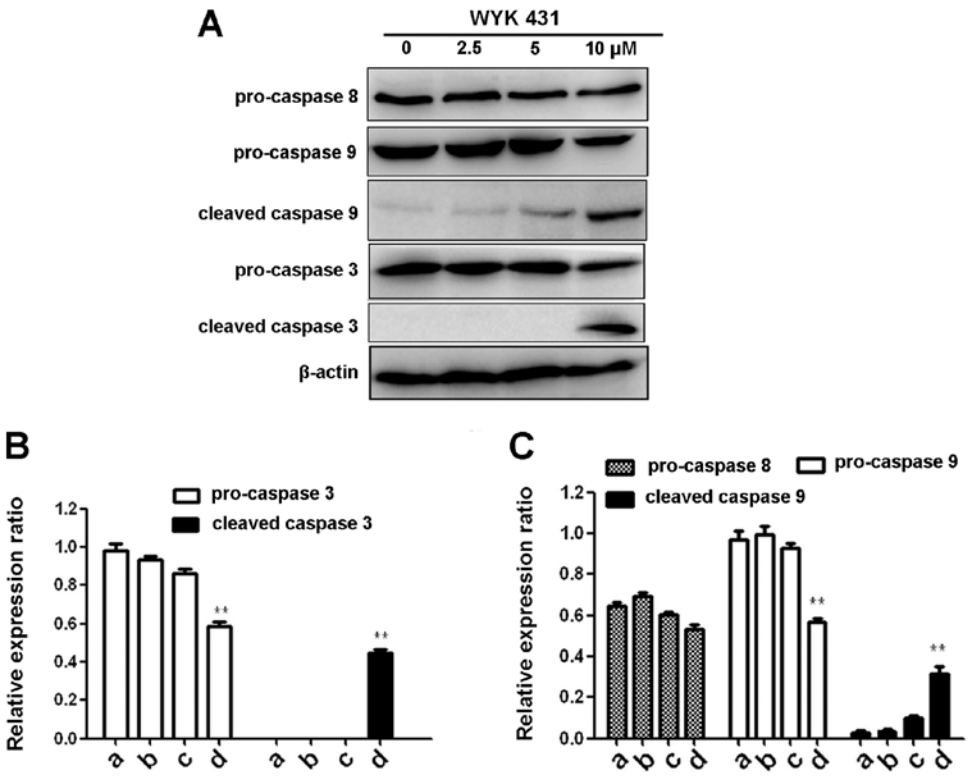

Figure 4. Effect of WYK431 on caspase activation. (A) Cells were treated with WYK431 at indicated concentrations for 24 h and the whole cell lysates were prepared and analyzed by immunoblotting. (B and C) Bars represent the densitometric intensity of the indicated protein bands, using image analyzing software. Results are representative of three individual experiments. Control (a), WYK431 2.5 μM (b), WYK431 5 μM (c), WYK431 10 μM (d). **P<0.01 vs. control.

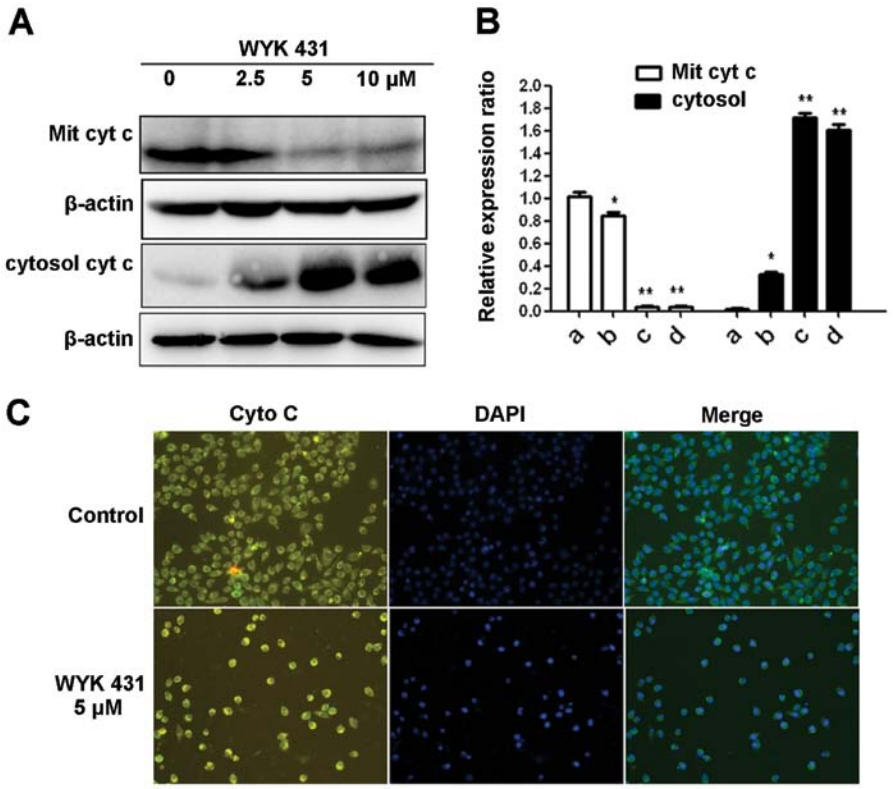

Figure 5. WYK431 induced cytochrome c release from mitochondria. (A) BGC823 cells were treated with WYK431 at indicated concentrations for 24 h and then the expression of cytochrome c in the mitochondrial and cytosol fraction was measured by western blotting. (B) Bars represent the densitometric intensity of the indicated protein bands, using image analyzing software. Results are representative of three individual experiments. Control (a), WYK431 2.5 μM (b), WYK431 5 μM (c), WYK431 10 μM (d). *P<0.05 and **P<0.01 vs. control. (C) WYK431 induced cytochrome c release from mitochondria. BGC823 cells were treated with WYK431 at indicated concentrations for 24 h and then the expression of cytochrome c in the mitochondrial and cytosol fraction was measured by immunofluorescence staining.

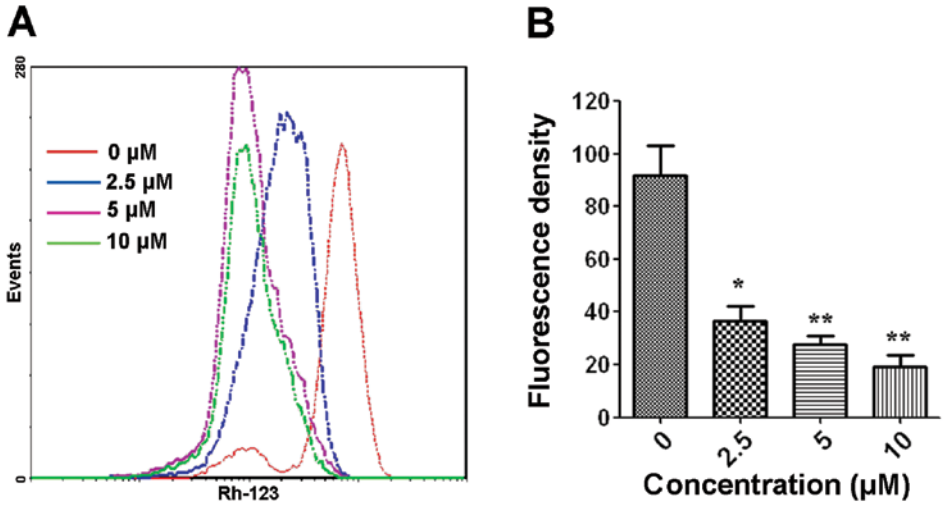

Figure 6. Reduction of the mitochondrial membrane potential by WYK431. (A) BGC823 cells were treated with WYK431 at indicated concentration for 24 h and were stained by Rh123 to determine the change of ΔΨm by flow cytometry. (B) Columns show the quantification of rhodamine 123 fluorescence. Data are expressed as means ± SD, n=3. *P<0.05 and **P<0.01, compared with control, one-way analysis of variance.

Table II. Quantification of apoptosis by Annexin V-FITC/PI staining.

Treatment (36 h)	Percentage ± standard deviation			
	AV^-/PI^-	AV^+/PI^-	AV^+/PI^+	AV^-/PI^+
Control	94.0±2.5	1.0±0.3	2.5±0.7	2.5±0.6
2.5 μM	83.7±5.8[a]	3.8±1.4	7.0±1.6[a]	5.5±1.4
5 μM	27.4±5.2[b]	45.1±4.2[b]	20.4±3.7[b]	7.1±2.0
10 μM	18.5±1.7[b]	53.7±2.1[b]	24.5±2.4[b]	3.3±0.7

[a]P<0.05 and [b]P<0.01, compared with control, one-way analysis of variance.

Table III. The final WBC parameters of different groups.

Types	Control	WYK431 5 mg/kg	WYK431 10 mg/kg	WYK431 20 mg/kg
LYM %	8.6±1.2	6.4±3.2	8.0±6.0	10.1±5.4
MON %	4.9±2.6	3.7±3.1	5.4±5.9	8.4±7.3
NEUT %	73.2±4.9	77.5±3.7	73.3±8.1	69.5±7.2
EOS %	10.5±2.8	10.2±2.6	10.9±3.3	10.2±5.5
BAS %	2.9±1.2	2.2±0.7	2.4±0.8	1.7±0.5

after treatment of BGC823 cells with WYK431 at indicated concentrations for 24 h, cytochrome c was detected in cytosolic fraction concentration-dependently, whereas a decreased level of cytochrome c was detected in mitochondria fraction (Fig. 5A and B). In addition, the release of cytochrome c from mitochondria into cytosol was visualized in WYK431-treated cells by fluorescence microscopy (Fig. 5C). Overall, these results indicated that WYK431 induced the release of cytochrome c from mitochondria into cytosol in BGC823 cells.

Effects of WYK431 on mitochondrial transmembrane potential. A key step in the intrinsic apoptotic pathway is the disruption of the mitochondrial membrane, which lead to loss mitochondrial transmembrane potential ΔΨm (37). It is an early event coinciding with caspase activation. To gain further insight into the mechanism underlying apoptosis induced by WYK431, we investigated whether WYK431 promotes mitochondrial disruption. Therefore, ΔΨm was examined by flow cytometry using the cationic lipophilic green fluorochrome rhodamine 123. Mitochondrial membrane permeability disruption is associated with a lack of rhodamine 123 retention and a decrease in fluorescence in intrinsic apoptosis pathway. Fig. 6 showed that WYK431 triggered the loss of mitochondrial transmembrane potential in BGC823 cells.

Effect of WYK431 on Bcl-2 and Bax expression. We measured Bcl-2 and Bax expression in BGC823 cells after WYK treatment for 24 h. Fig. 7 shows that WYK431 treatment led to an increased level of Bax in BGC823 cells, but no significant change of Bcl-2 was observed. The result was coincident with the result of cytochrome c release. Collectively, we propose that WYK431 promotes apoptosis through the intrinsic pathway.

Effects of WYK431 on the PI3K/Akt signaling pathways. To investigate the effect of WYK431 on PI3K/Akt pathway, the expression level of PI3K and its downstream components in BGC823 cells after WYK431 treatment for 8 h were detected by western blot analysis. Our data indicated that exposure of BGC823 cells to WYK431 markedly decreased the expression levels of PI3K p110α and p85 proteins (Fig. 8). Akt, the downstream target of PI3K, plays a crucial role in carcinogenesis and cancer development. Our result showed that the expression of p-Akt (473), as the active form of Akt, substantially decreased after WYK431 treatment. However, the level of total Akt was unaffected by WYK431.

Antitumor activity of WYK431 in vivo. To evaluate the antitumor activity of WYK431 *in vivo*, BGC823 bearing BALB/c

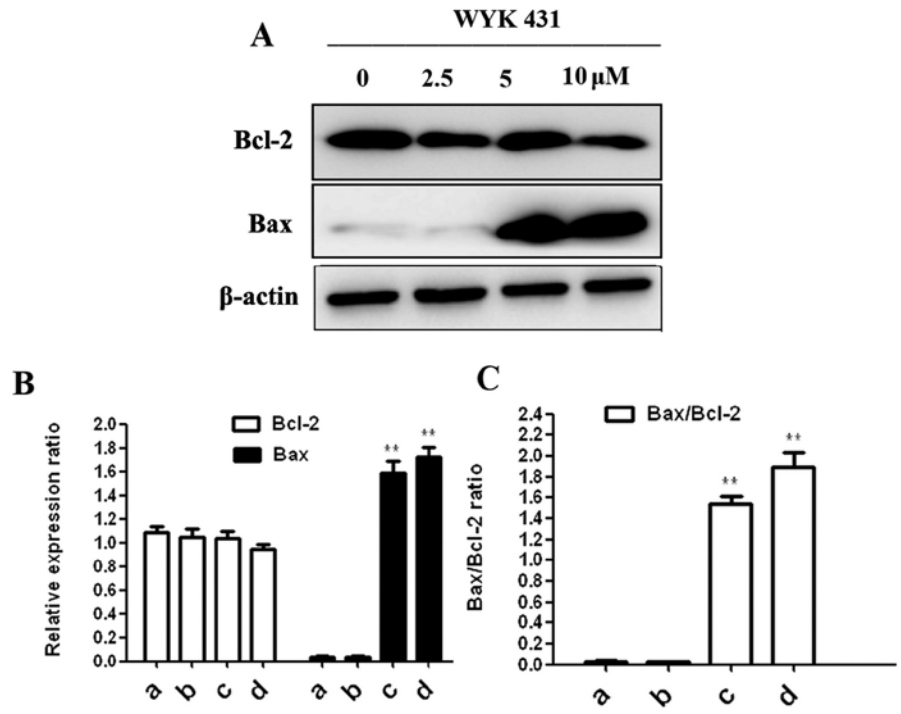

Figure 7. Effect of WYK431 on Bax and Bcl-2 expression. (A) Cells were treated with WYK431 at indicated concentrations for 24 h and the whole cell lysates were prepared and analyzed by immunoblotting. (B) Bars represent the densitometric intensity of the indicated protein bands, using image analyzing software. Results are representative of three individual experiments. Control (a), WYK431 2.5 μM (b), WYK431 5 μM (c), WYK431 10 μM (d). *P<0.05 and **P<0.01 vs. control. (C) Bars represent the ratio of Bax to Bcl-2. Control (a), WYK431 2.5 μM (b), WYK431 5 μM (c), WYK431 10 μM (d). *P<0.05 and **P<0.01 vs. control.

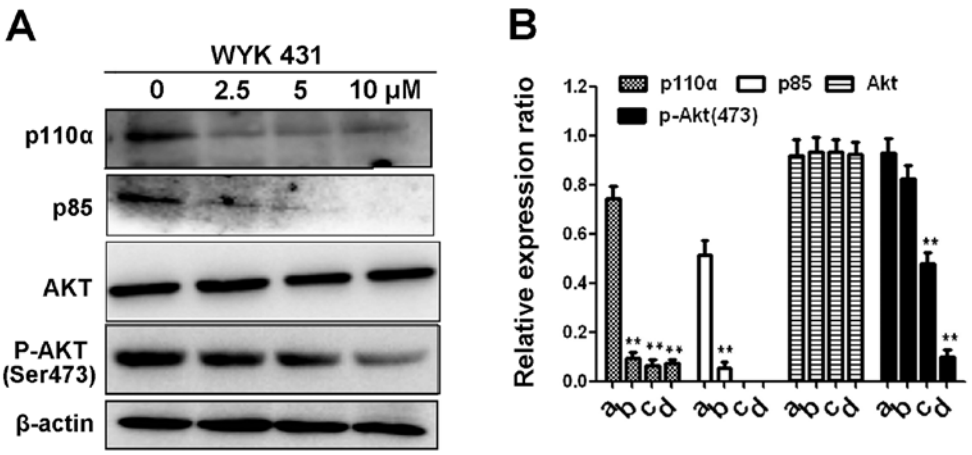

Figure 8. WYK431 blocks the PI3K/Akt pathway. (A) Effect of WYK431 on p110α, p85, Akt, p-Akt (473) in BGC823 cells. Cells were treated with indicated concentrations for 8 h and the whole cell lysates were prepared and analyzed by western blotting. (B) Bars represent the densitometric intensity of the indicated protein bands, using image analyzing software. Results are representative of three individual experiments. Control (a), WYK431 2.5 μM (b), WYK431 5 μM (c), WYK431 10 μM (d). **P<0.01 vs. control.

nude mice were treated with vehicle, 5, 10 and 20 mg/kg of WYK431, respectively. WYK431 exhibited a significant antitumor activity in inhibiting tumor progression compared with vehicle-treated animals. As noted in Fig. 9A, WYK431 administered at 5, 10 and 20 mg/kg of WYK431 suppressed tumors 28.4, 41.9, 63.6%, compared with vehicle-treated animals (P<0.05). Moreover, WYK431 treatment was well tolerated, with only small effects on body weight, which was consistent with the notion that WYK431 preferably targets tumor cells and thus exhibited little toxicity (Fig. 9B). Hematological analysis showed that WYK431 did not significantly decrease the number of white blood corpuscles (Table III).

Histological analysis by TUNEL. The tumors were removed and TUNEL assay was performed. Five equal-sized fields were randomly chosen and analyzed in tumor sections. We observed more TUNEL-positive cells with dark green fluorescent staining in the treatment group, indicating a significant increased apoptosis in the treatment group compared with control group (Fig. 9C). These results suggest that WYK431 induced apoptosis of tumor cells *in vivo*.

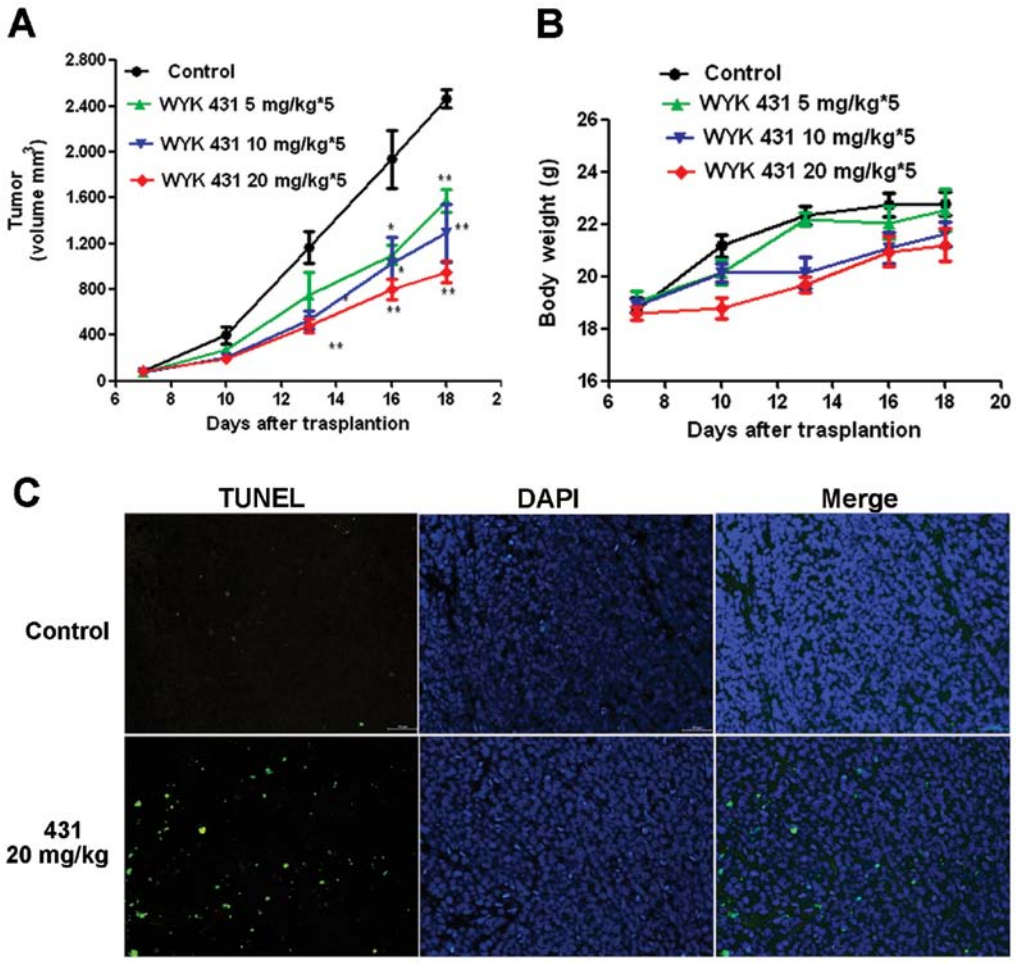

Figure 9. Effects of WYK431 on the growth of xenografts and TUNEL assay *in vivo*. WYK431 inhibited the growth of established BGC823 tumor xenografts in the athymic nude mice. (A) Tumor volume of BGC823 was measured on the indicated days. (B) Body weight of mice with BGC823 tumor xenografts were measured in the indicated days. (C) Three independent tumors were evaluated from the control group or WYK431-treated group for apoptotic measure using TUNEL assay.

Discussion

Quinazoline derivatives possess significant antitumor effects via inducing apoptosis and cell cycle arrest (31,38). WYK431, a novel quinazoline derivative, is a highly potent and broad spectrum anticancer compound, and BGC823 cells were the most sensitive. To our knowledge, this study is the first to demonstrate that WYK431 possesses significant antitumor activities through inducing G_2/M phase arrest and apoptosis by blocking the PI3K signaling pathway in human gastric cancer cells *in vitro*. Moreover, it inhibits tumor growth *in vivo* as well.

Hallmarks of cancer include an uncontrolled cell cycle and resistance to apoptosis signals (39). Therefore, the induction of apoptosis and cell cycle blockage are important cancer prevention treatment goals. Cell cycle arrest is a critical mechanism of anticancer drug suppressing cell proliferation (40). Cell cycle is promoted by a number of proteins including cyclin dependent kinases (CDKs) and cyclins. In G_2 phase, cells synthesize cyclin A/cyclin B, which can form a complex with CDK1 to promote entry into mitosis (41). When the CDK1/cyclin B or cyclin A complex initially forms, it is maintained in the inactive form by phosphorylation at two sites, threonine 14 and tyrosine 15 (42). Cdc25C can dephosphorylate Cdk1 at threonine 14 and tyrosine 15 and activate CDK1-cyclin B or CDK1-cyclin A complex. The activated CDK1-cyclin B or CDK1-cyclin A complex translocate into nucleus at the G_2/M checkpoint to promote cell entry into mitosis (43,44). Therefore, we investigated the effect of WYK431 on the cell cycle. Our result showed that treatment of BGC823 with WYK431 for 24 h caused cells to accumulate in G_2/M phase which was associated with downregulation of CDK1 and Cdc25C proteins. PI3K/AKT pathway has been implicated in cell cycle progression (45). Inhibited PI3K/AKT pathway regulated the expression of CDKs and cyclins, eventually causing G_2/M arrest (46-48). In the present study, we observed that WYK431-mediated downregulation of cell cycle regulatory molecular may be associated with the decrease of p110α and p85. Further studies are required to investigate the detailed mechanism of how PI3K/Akt pathway regulates WYK431-induced G_2/M arrest in BGC823 cells.

Apoptosis is the most common way that antitumor agents induce cell death (49,50). Hoechst staining and FCM analysis showed that WYK431 induced BGC823 cells apoptosis. Our study also demonstrated that WYK431 could induce tumor cell apoptosis by TUNEL assay. In order to explore the mechanism of apoptosis induced by WYK431, we examined the proteins involved in apoptosis. Our results showed that

caspase-3 was activated by WYK431. There are two main pathway of apoptosis, the death receptor (extrinsic) pathway and mitochondria (intrinsic) pathway. Activation of caspase-3 is in either one of the pathways (51). To determine the pathway of apoptosis induced by WYK431, caspase-8 and caspase-9 involved in the extrinsic and intrinsic pathway, respectively, was detected (52). We found that caspase-9, but not caspase-8 was activated by WYK431, indicating that WYK431 induces BGC823 cell apoptosis via intrinsic pathway. The disruption of mitochondrial membrane potential and the release of cytochrome c from mitochondria into cytoplasm are recognized as key step in the mitochondria pathway.

Our results showed that the treatment of BGC823 cells with WYK431 led to a loss of $\Delta\Psi m$ and released cytochrome c from mitochondria into cytoplasm, indicating an activation of the intrinsic apoptosis pathway. The process is regulated by Bcl-2 family proteins which include proapoptotic members such as Bax and anti-apoptotic members such as Bcl-2 (53). Bcl-2 family members located on the mitochondrial membrane can alter the permeability of the mitochondrial membrane and trigger the release of cytochrome c. To further confirm the involvement of the mitochondrial pathway in WYK431 induced apoptotic death, the expression of Bax and Bcl-2 were detected. The expression of Bax was increased in cells treated with WYK431, whereas there was no change in Bcl-2 protein expression. Thus, the ratio of Bax to Bcl-2 was altered. We assume that upregulation of Bax may be involved in the release of cytochrome c from mitochondria into cytosol after WYK431 treatment.

Many studies showed that inactivation of Akt by dephosphorylation play a key role in tumor suspression (54,55). Our results show that WYK431 could inhibit Akt phosphorylation. It is well-established that the inhibition of PI3K/Akt signal pathway can induce apoptosis of cancer cells (56). Our investigations revealed that treatment with WYK431 remarkably decreased Akt phosphorylation and promote cell apoptosis indicating that PI3K/Akt pathway is involved in WYK431-induced apoptosis. These results suggest that PI3K/Akt is involved in apoptosis induced by WYK431.

In conclusion, this is the first study reporting that WYK431 exerts potential anti-proliferative effect against BGC823 cells probably through cell cycle arrest and the mitochondria apoptotic pathway. Our studies show that WYK431 treatment blocks the PI3K/Akt pathways. In addition, the *in vivo* study showed that WYK431 can suppress tumor growth of BGC823 cells without obvious toxicity, indicating that WYK431 provide chemical structure information that can be used for the design and development of more effective derivatives.

Acknowledgements

We thank Ms. Furong Zhang and Hanze Yang for technical assistance and Professor Bailing Xu for providing compound 431. This study was supported by the National Natural Science Foundation (Grant no. 81273380).

References

1. Kamangar F, Dores GM and Anderson WF: Patterns of cancer incidence, mortality, and prevalence across five continents: defining priorities to reduce cancer disparities in different geographic regions of the world. J Clin Oncol 24: 2137-2150, 2006.
2. Crew KD and Neugut AI: Epidemiology of gastric cancer. World J Gastroenterol 12: 354-362, 2006.
3. Wagner AD, Grothe W, Behl S, *et al*: Chemotherapy for advanced gastric cancer. Cochrane Database Syst Rev 2: CD004064, 2005.
4. Van Cutsem E, Moiseyenko VM, Tjulandin S, *et al*: Phase III study of docetaxel and cisplatin plus fluorouracil compared with cisplatin and fluorouracil as first-line therapy for advanced gastric cancer: a report of the V325 Study Group. J Clin Oncol 24: 4991-4997, 2006.
5. Vivanco I and Sawyers CL: The phosphatidylinositol 3-Kinase AKT pathway in human cancer. Nat Rev Cancer 2: 489-501, 2002.
6. Vanhaesebroeck B, Guillermet-Guibert J, Graupera M and Bilanges B: The emerging mechanisms of isoform-specific PI3K signalling. Nat Rev Mol Cell Biol 11: 329-341, 2010.
7. Paweletz CP, Charboneau L, Bichsel VE, *et al*: Reverse phase protein microarrays which capture disease progression show activation of pro-survival pathways at the cancer invasion front. Oncogene 20: 1981-1989, 2001.
8. Bellacosa A, Kumar CC, Di Cristofano A and Testa JR: Activation of AKT kinases in cancer: implications for therapeutic targeting. Adv Cancer Res 94: 29-86, 2005.
9. Testa JR and Bellacosa A: AKT plays a central role in tumorigenesis. Proc Natl Acad Sci USA 98: 10983-10985, 2001.
10. Liu P, Cheng H, Roberts TM and Zhao JJ: Targeting the phosphoinositide 3-kinase pathway in cancer. Nat Rev Drug Discov 8: 627-644, 2009.
11. Engelman JA, Luo J and Cantley LC: The evolution of phosphatidylinositol 3-kinases as regulators of growth and metabolism. Nat Rev Genet 7: 606-619, 2006.
12. Cantley LC: The phosphoinositide 3-kinase pathway. Science 296: 1655-1657, 2002.
13. Lee JW, Soung YH, Kim SY, *et al*: PIK3CA gene is frequently mutated in breast carcinomas and hepatocellular carcinomas. Oncogene 24: 1477-1480, 2005.
14. Campbell IG, Russell SE, Choong DY, *et al*: Mutation of the PIK3CA gene in ovarian and breast cancer. Cancer Res 64: 7678-7681, 2004.
15. Li VS, Wong CW, Chan TL, *et al*: Mutations of PIK3CA in gastric adenocarcinoma. BMC Cancer 5: 29, 2005.
16. Bachman KE, Argani P, Samuels Y, *et al*: The PIK3CA gene is mutated with high frequency in human breast cancers. Cancer Biol Ther 3: 772-775, 2004.
17. Duronio V, Scheid MP and Ettinger S: Downstream signalling events regulated by phosphatidylinositol 3-kinase activity. Cell Signal 10: 233-239, 1998.
18. Blume-Jensen P and Hunter T: Oncogenic kinase signalling. Nature 411: 355-365, 2001.
19. Johnson DG and Walker CL: Cyclins and cell cycle checkpoints. Annu Rev Pharmacol Toxicol 39: 295-312, 1999.
20. Senderowicz AM and Sausville EA: Preclinical and clinical development of cyclin-dependent kinase modulators. J Natl Cancer Inst 92: 376-387, 2000.
21. Kasibhatla S and Tseng B: Why target apoptosis in cancer treatment? Mol Cancer Ther 2: 573-580, 2003.
22. Jemal A, Siegel R, Ward E, *et al*: Cancer statistics, 2008. CA Cancer J Clin 58: 71-96, 2008.
23. Plenchette S, Filomenko R, Logette E, *et al*: Analyzing markers of apoptosis in vitro. Methods Mol Biol 281: 313-331, 2004.
24. Hengartner MO: The biochemistry of apoptosis. Nature 407: 770-776, 2000.
25. Sartorius U, Schmitz I and Krammer PH: Molecular mechanisms of death-receptor-mediated apoptosis. Chembiochem 2: 20-29, 2001.
26. Jiang X and Wang X: Cytochrome c promotes caspase-9 activation by inducing nucleotide binding to Apaf-1. J Biol Chem 275: 31199-31203, 2000.
27. Wakeling AE, Guy SP, Woodburn JR, *et al*: ZD1839 (Iressa): an orally active inhibitor of epidermal growth factor signaling with potential for cancer therapy. Cancer Res 62: 5749-5754, 2002.
28. Baba A, Kawamura N, Makino H, Ohta Y, Taketomi S and Sohda T: Studies on disease-modifying antirheumatic drugs: synthesis of novel quinoline and quinazoline derivatives and their anti-inflammatory effect. J Med Chem 39: 5176-5182, 1996.
29. Rohini R, Muralidhar Reddy P, Shanker K, Hu A and Ravinder V: Antimicrobial study of newly synthesized 6-substituted indolo[1,2-c]quinazolines. Eur J Med Chem 45: 1200-1205, 2010.
30. Honkanen E, Pippuri A, Kairisalo P, Nore P, Karppanen H and Paakkari I: Synthesis and antihypertensive activity of some new quinazoline derivatives. J Med Chem 26: 1433-1438, 1983.

31. Jin J, Zhu L-N, Zhang H-J, *et al*: XLN306 induces apoptosis in human breast carcinoma MX-1 cells. Acta Pharm Sin B 1: 84-88, 2011.
32. Wang YK, Jin J, Zhu LN, *et al*: Synthesis and antitumor activity of novel 2-(1-substituted-piperidin-4-ylamino)quinazolines as antitumor agents. Yao Xue Xue Bao 47: 1164-1178, 2012.
33. Scaduto RC Jr and Grotyohann LW: Measurement of mitochondrial membrane potential using fluorescent rhodamine derivatives. Biophys J 76: 469-477, 1999.
34. Konopleva M, Contractor R, Tsao T, *et al*: Mechanisms of apoptosis sensitivity and resistance to the BH3 mimetic ABT-737 in acute myeloid leukemia. Cancer Cell 10: 375-388, 2006.
35. Lewis JS, Meeke K, Osipo C, *et al*: Intrinsic mechanism of estradiol-induced apoptosis in breast cancer cells resistant to estrogen deprivation. J Natl Cancer Inst 97: 1746-1759, 2005.
36. Nunez G, Benedict MA, Hu Y and Inohara N: Caspases: the proteases of the apoptotic pathway. Oncogene 17: 3237-3245, 1998.
37. Green DR and Reed JC: Mitochondria and apoptosis. Science 281: 1309-1312, 1998.
38. Cubedo E, Cordeu L, Bandres E, *et al*: New symmetrical quinazoline derivatives selectively induce apoptosis in human cancer cells. Cancer Biol Ther 5: 850-859, 2006.
39. Hanahan D and Weinberg RA: Hallmarks of cancer: the next generation. Cell 144: 646-674, 2011.
40. Shapiro GI and Harper JW: Anticancer drug targets: cell cycle and checkpoint control. J Clin Invest 104: 1645-1653, 1999.
41. von Bergwelt-Baildon MS, Kondo E, Klein-Gonzalez N and Wendtner CM: The cyclins: a family of widely expressed tumor antigens? Expert Rev Vaccines 10: 389-395, 2011.
42. Goss VL, Cross JV, Ma K, Qian Y, Mola PW and Templeton DJ: SAPK/JNK regulates cdc2/cyclin B kinase through phosphorylation and inhibition of cdc25c. Cell Signal 15: 709-718, 2003.
43. Karlsson-Rosenthal C and Millar JB: Cdc25: mechanisms of checkpoint inhibition and recovery. Trends Cell Biol 16: 285-292, 2006.
44. Galea CA, Wang Y, Sivakolundu SG and Kriwacki RW: Regulation of cell division by intrinsically unstructured proteins: intrinsic flexibility, modularity, and signaling conduits. Biochemistry 47: 7598-7609, 2008.
45. Chang F, Lee JT, Navolanic PM, *et al*: Involvement of PI3K/Akt pathway in cell cycle progression, apoptosis, and neoplastic transformation: a target for cancer chemotherapy. Leukemia 17: 590-603, 2003.
46. Wang J, Wu A, Xu Y, Liu J and Qian X: M(2)-A induces apoptosis and G(2)-M arrest via inhibiting PI3K/Akt pathway in HL60 cells. Cancer Lett 283: 193-202, 2009.
47. Yuan Q, Cai S, Zhang X, *et al*: A new protoapigenone analog RY10-4 induces apoptosis and suppresses invasion through the PI3K/Akt pathway in human breast cancer. Cancer Lett 324: 210-220, 2012.
48. Li Y, Zhang P, Qiu F, *et al*: Inactivation of PI3K/Akt signaling mediates proliferation inhibition and G_2/M phase arrest induced by andrographolide in human glioblastoma cells. Life Sci 90: 962-967, 2012.
49. Xu YZ, Zheng RL, Zhou Y, *et al*: Small molecular anticancer agent SKLB703 induces apoptosis in human hepatocellular carcinoma cells via the mitochondrial apoptotic pathway in vitro and inhibits tumor growth in vivo. Cancer Lett 313: 44-53, 2011.
50. Sun B, Geng S, Huang X, *et al*: Coleusin factor exerts cytotoxic activity by inducing G_0/G_1 cell cycle arrest and apoptosis in human gastric cancer BGC-823 cells. Cancer Lett 301: 95-105, 2011.
51. Ferreira CG, Epping M, Kruyt FA and Giaccone G: Apoptosis: target of cancer therapy. Clin Cancer Res 8: 2024-2034, 2002.
52. Adams JM and Cory S: The Bcl-2 protein family: arbiters of cell survival. Science 281: 1322-1326, 1998.
53. Youle RJ and Strasser A: The BCL-2 protein family: opposing activities that mediate cell death. Nat Rev Mol Cell Biol 9: 47-59, 2008.
54. Brognard J, Clark AS, Ni Y and Dennis PA: Akt/protein kinase B is constitutively active in non-small cell lung cancer cells and promotes cellular survival and resistance to chemotherapy and radiation. Cancer Res 61: 3986-3997, 2001.
55. Martelli AM, Tazzari PL, Tabellini G, *et al*: A new selective AKT pharmacological inhibitor reduces resistance to chemotherapeutic drugs, TRAIL, all-trans-retinoic acid, and ionizing radiation of human leukemia cells. Leukemia 17: 1794-1805, 2003.
56. Hussain AR, Al-Rasheed M, Manogaran PS, *et al*: Curcumin induces apoptosis via inhibition of PI3'-kinase/AKT pathway in acute T cell leukemias. Apoptosis 11: 245-254, 2006.